

Procaine Detection Using Hybrids of Cobalt-Metalloporphyrin with Gold and Silver Nanoparticles

¹Anca Lascu*, ¹Anca Palade, ²Mihaela Birdeanu and ¹Eugenia Fagadar-Cosma

¹*Institute of Chemistry Timisoara of Romanian Academy, 24 M. Viteazul Ave., 300223-Timisoara, Romania.*

²*National Institute for Research and Development in Electrochemistry and Condensed Matter, 1 Plautius Andronescu Street, 300224-Timisoara, Romania.*

ancalascu@yahoo.com*

(Received on 16th May 2017, accepted in revised form 13th June 2018)

Summary: Two organic-inorganic nanomaterials derived from Co(II)-tetra(3-hydroxyphenyl)porphyrin (*Co-3OHPP*) and noble metal nanoparticles, namely: Co-porphyrin-nanoAu (*Co-3OHPP/nAu*) and Co-porphyrin-nanoAg (*Co-3OHPP/nAg*) were obtained and tested for their capacity to detect procaine. Both hybrids present changes in UV-vis spectroscopy after interaction with procaine, in the same range of procaine concentration. The silver colloid is more easily obtainable and more economically affordable and its hybrid has a wider range of procaine detection from $5.39 \times 10^{-5} \text{ mol l}^{-1}$ to $28.04 \times 10^{-5} \text{ mol l}^{-1}$ concentration, thus being useful for the monitoring of the anesthetic remanence in patients' plasma. Besides, the plasmonic band of the hybrid is more clearly defined. AFM studies were performed to compare the morphology of the two hybrid materials, *Co-3OHPP/nAu* and *Co-3OHPP/nAg* after being exposed to procaine. Both materials display triangular geometries that in case of *Co-3OHPP/nAg* are not very well defined taking also the form of *kvatarons* and these two coexisting forms generate pyramidal architectures.

Keywords: Co(II)-porphyrin; Gold and silver hybrids; Anesthetic detection; UV-vis spectrophotometry; AFM.

Introduction

Procaine, scientifically known as: 2-diethylaminoethyl *p*-aminobenzoate monohydrochloride, is a cheap short-acting local anesthetic. The process of anesthesia is of higher quality and the duration is increased when procaine is coadministered with a vasoconstrictor that helps to reduce bleeding. Besides, the amount of anesthetic required is reduced [1]. This drug is also used for relieving arthritis, "hardening of the arteries" in the brain (cerebral atherosclerosis) [2, 3], dementia [4], depression, hair loss, high blood pressure, and sexual performance problems [5]. Ana Aslan [6], a Romanian researcher, recognized for her priorities in Geriatrics, used procaine as primary ingredient in the preparation Gerovital H3 [7], a product used for relieving the effects of aging. Procaine has the ability to stabilize the cardiac rhythm after cardiac surgery by reducing the need for synchronized direct current (DC) shock to obtain sinus rhythm [8]. Steroid and procaine hydrochloride injections are effective in carpal tunnel syndrome (CTS) treatment but alone it was found to be also effective in patients with diabetes mellitus for whom steroid use is contraindicated [9].

Although procaine has no apparent side effects in lower concentrations than 1 mM its accurate dosage is required in medical investigations [9].

Procaine hydrochloride was detected by a colorimetric method based on measurement of the intensity of the orange-red color produced by the reaction with 1,2-naphthoquinone-4-sulfonic acid sodium salt in aqueous solution [10]. This method is suited for routine analysis of pharmaceutical preparations of procaine hydrochloride due to its simplicity, sensitivity, and accuracy.

Procaine hydrochloride was determined also by potentiometric titration with cerium (IV) sulfate solution in sulfuric acid. The procaine was determined in geriatrics pharmaceuticals in the concentration range from $10^{-2} \text{ mol} \cdot \text{l}^{-1}$ to $10^{-4} \text{ mol} \cdot \text{l}^{-1}$ [11].

A better performance of the procaine detection in the range was from 8.3×10^{-8} to $5.0 \times 10^{-3} \text{ mol l}^{-1}$ with a detection limit of $8.3 \times 10^{-8} \text{ mol l}^{-1}$ was obtained by a sensor fabricated from an Ag-electrode modified with a PVC membrane containing procaine tetraphenylborate [12].

Recently, procaine and lidocaine were reported to be determined by high performance liquid chromatography (HPLC) detection incorporating resonance Rayleigh scattering (RRS) [13]. The weak intensity of procaine and lidocaine was enhanced by the addition of a dye, namely Erythrosin, in acidic medium. The limit of detection for procaine was 2.3

*To whom all correspondence should be addressed.

mg l⁻¹ and for lidocaine 15 mg l⁻¹. The method was validated for the detection of procaine and lidocaine in human plasma samples.

A spectrophotometric method using 7-iodo-8-hydroxyquinoline 5-sulphonic acid as chromophore for the determination of procaine by diazotization-coupling reaction was found useful [14]. Acidic medium improved the diazotization reaction and a basic environment increased the developing of a more intense color. The method proved to be accurate, effortless and cheap.

A procaine sensitive membrane was prepared by spin-coating, using as substrate TiO₂ thin films. A pH electrode was constructed and the concentration of procaine in Chinese herbal medicine was detected. The procaine concentration range detectable by this pH electrode varied between 1.0 x 10⁻² mol l⁻¹ and 1.0 x 10⁻⁶ mol l⁻¹ [15].

Besides beneficial effects, the development of a large variety of anesthetics has unfortunately the disadvantage of possible fatal intoxications caused by their combination. Procaine, mepivacaine, lidocaine, ropivacaine, oxybuprocaine, tetracaine, bupivacaine, T-caine and dibucaine are local anesthetics that were reported [16] to be simultaneously detected by a high-performance liquid chromatography–tandem mass spectrometry method.

Using chlorprocaine 3% as local anesthetic was reported to provide the advantage of earlier discharge of patients undergoing minor orthopedic surgery [17]. The lowering of costs for nursing interventions and overall care was thus accomplished.

Cobalt-metalloporphyrins are well-known for their rich supramolecular chemistry and their capacity to act as building blocks when linked with other organic or inorganic molecules in order to obtain electrocatalytic materials useful in detection [18]. The optical and catalytic properties are based on one hand on porphyrin redox versatility and on the other hand on the redox chemistry of Co(II) that can be converted into a more nucleophilic Co(I) species by single-electron reduction process [19]. For example, Co(III)-tetrakis(4-aminophenyl)porphyrin was electropolymerized together with *ortho*-phenyldiamine and used to measure the free sulfite concentration in red wine [20]. The same Co-metalloporphyrin imprinted in a copolymer matrix was sensitive to amperometric and potentiometric

detection of a toxic organohalide in the micromolar range [21]. Alternative thin film layers of β -substituted cobalt bis-porphyrin derivative and gold obtained by Langmuir–Schäfer method were successfully used for the detection of volatile organic compounds (VOCs) especially alcohols [22]. Another Co-porphyrin, namely: Co(II)-5-(4-carboxyphenyl),10,15,20-triphenylporphyrin, homogeneously dispersed into the SnO₂ oxide by sol-gel method proved to be sensitive towards the detection of methanol [23].

A hybrid nanomaterial, obtained from Co(II) 5,10,15,20-meso-tetra(3-hydroxyphenyl)porphyrin and gold nanoparticles was used for optical and electrochemical detection of hydrogen peroxide having potential in early medical diagnosis. Hydrogen peroxide concentration levels of (5–35 μ mol l⁻¹) were detected [24].

The use of silver and gold colloids in the obtaining of porphyrin-anorganic hybrid materials is known to produce wide band absorption in ultraviolet and visible domain [25].

The main purpose of this research was to obtain two different organic-inorganic nanomaterials namely: Co(II)-tetra(3-hydroxyphenyl)porphyrin-nano Au (*Co-3OHPP/nAu*) and Co(II)-tetra(3-hydroxyphenyl)porphyrin-nano Ag (*Co-3OHPP/nAg*) and to test their sensitivity to procaine (Fig. 1). The influence of noble metal nanoparticles upon the effectiveness of procaine detection by the two metalloporphyrin hybrids was compared.

Experimental

UV-vis spectra were recorded on a JASCO UV-visible spectrometer, model V-650, in various solvents (THF, THF-aqueous system) in 1 cm length quartz cuvettes. AFM images were obtained on a Nanosurf® Easy Scan 2 Advanced Research AFM apparatus, in ambient conditions. Silica plates were used for obtaining of samples by drop casting.

The gold colloid, the Co-porphyrin and the silver colloid were obtained according to previously reported papers [24, 26].

Procaine hydrochloride was acquired from Biesterfeld AG. Tetrahydrofurane (THF) was purchased from Merck and used without further purification.

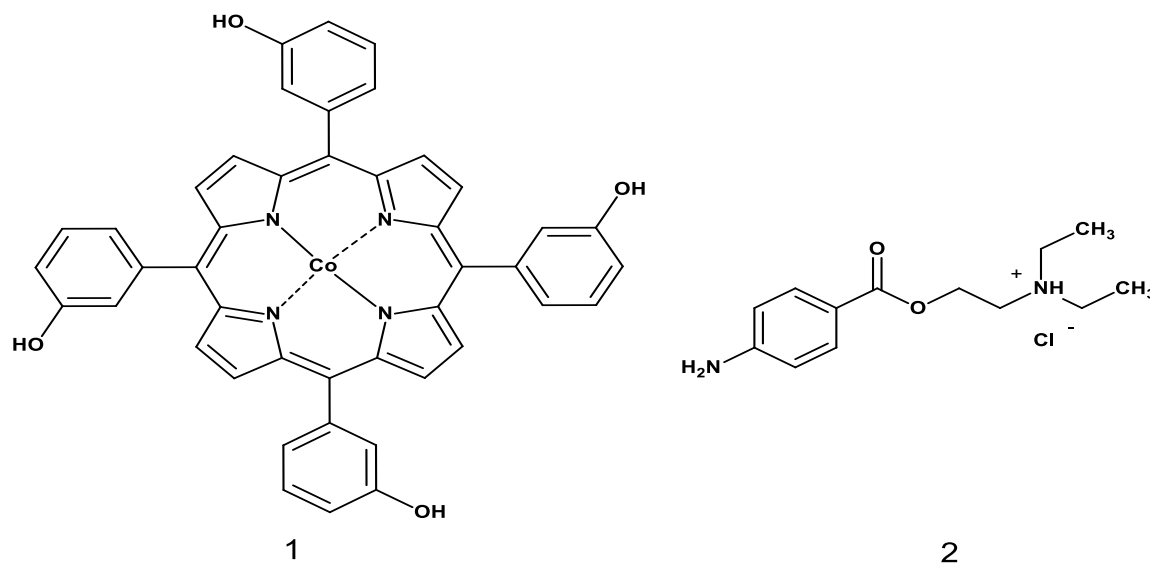


Fig. 1: Structures of *Co-3OHPP* porphyrin (a) and of procaine hydrochloride (b).

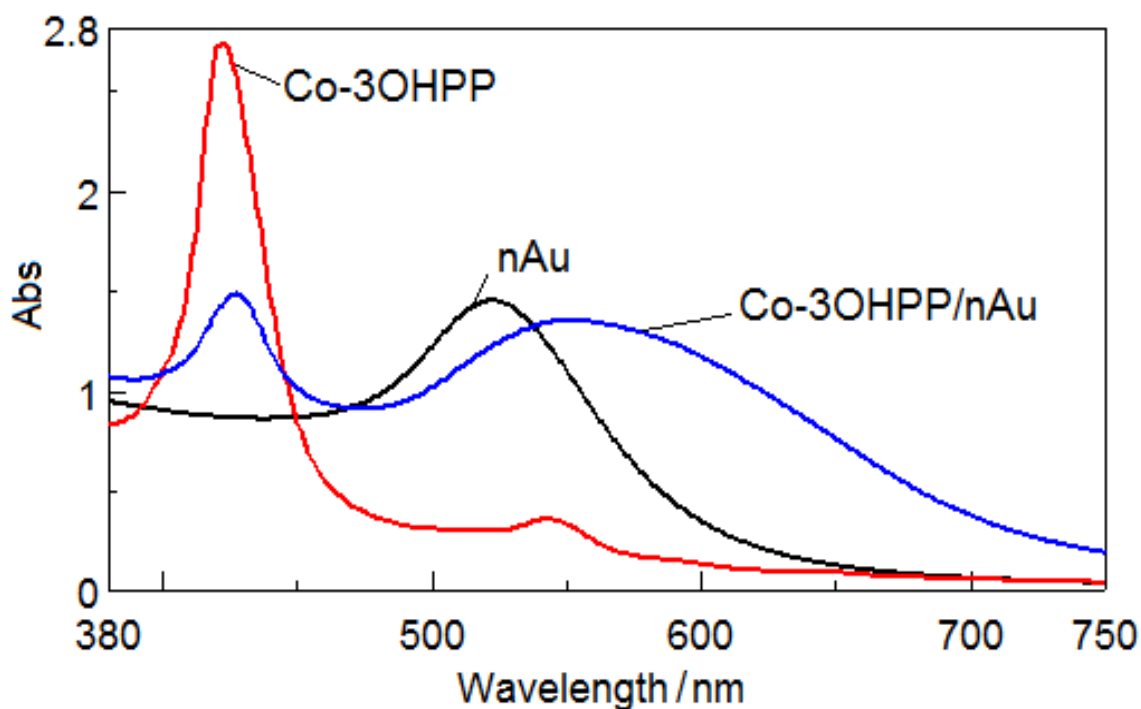


Fig. 2: Overlapped UV-vis spectra of the Co-porphyrin, nano-Au and *Co-3OHPP/nAu* hybrid.

Obtaining of Co-3OHPP/nAu hybrid:

Co-3OHPP/nAu hybrid was prepared as previously reported [24]. A solution of Co(II)-tetra(3-hydroxyphenyl)porphyrin in THF (1 ml, $c = 5.149 \times 10^{-5} \text{ mol l}^{-1}$) was added to 3 ml gold colloid solution ($c = 4.58 \times 10^{-4} \text{ mol l}^{-1}$), under vigorous stirring.

Obtaining the Co-3OHPP/nAg hybrid:

The *Co-3OHPP* porphyrin solution in THF ($c = 2.9905 \times 10^{-3} \text{ mol l}^{-1}$) was acidified to pH = 3 with 0.01 M HCl solution. The concentration of the silver colloidal solution was ($c = 1.562 \times 10^{-4} \text{ mol l}^{-1}$). The hybrid was obtained by adding to 3 ml silver colloid the acidified solution of *Co-3OHPP*

metalloporphyrin in portions of 20 μl up to sample 10 and portions of 50 μl up to sample 18. The stability domain of the hybrid covers concentrations of Co-3OHPP from $0.643 \times 10^{-6}\text{M}$ to $8.138 \times 10^{-6}\text{M}$. The material used for sensing applications was the hybrid that had the Co-3OHPP concentration of $1.577 \times 10^{-6}\text{M}$.

Results and Discussion

UV-vis spectroscopy

The *Co-3OHPP-nAu* hybrid formed was analyzed by UV-vis spectroscopy (Fig. 2) and presents an intense and wide absorption band that is bathochromically shifted in comparison with the bare gold plasmon. It can be observed from Fig. 2 that the absorption domain of the *Co-3OHPP/nAu* hybrid is extended from 400 nm to 700 nm, much wider than each of the absorptions of the starting materials.

Based on the knowledge that the silver colloidal particles possess a surface negative charge, the acidifying of the metalloporphyrin, in the limits of non producing the demetalation, can facilitate the obtaining of the *Co-3OHPP/nAg* hybrid (Fig. 3). The *Co-3OHPP/nAg* hybrid presents a larger plasmonic band than the initial silver colloidal solution, but the absorption domain does not increase as much as in the case of the hybrid formed with gold colloid. Two isosbestic points are visible (Fig. 3a,b), one located at 300 nm and another one at 525 nm. The first one points out the formation of the complex between

porphyrin and Ag nanoparticles and the second one is in connection with the strong shifting to the red of the hybrid band and producing its widening up to 650 nm, probably due to an electrostatic equilibrium between materials with opposite charges. Based on the fact that we compensate the negative charges at the surface of the silver plasmon by acidifying the system, the red shift visible in the range of 600 – 700 nm might be explained by a charge transfer transition between the porphyrin donor and the neutral surface of the silver plasmon [24]. Dispersion forces can play an important role as well. The presence of four hydroxyl groups on each Co-3OHPP metalloporphyrin are likely to create multiple hydrogen bonds in several directions.

Analysing the spectra, we chose the *Co-3OHPP/nAg* hybrid having the Co-3OHPP concentration of $1.577 \times 10^{-6}\text{M}$, that presents the widest absorption band, to be tested for procaine detection.

Procaine detection by *Co-3OHPP/nAu* and *Co-3OHPP/nAg* hybrids

A solution of procaine chlorhydrate 0.1% in water ($4.23 \times 10^{-3}\text{mol l}^{-1}$) was prepared. Portions of 20 μl from this solution were stepwise added to 3 ml solution of each hybrid material. The mixture was stirred for 30 seconds and then the UV-vis spectra were recorded for each step.

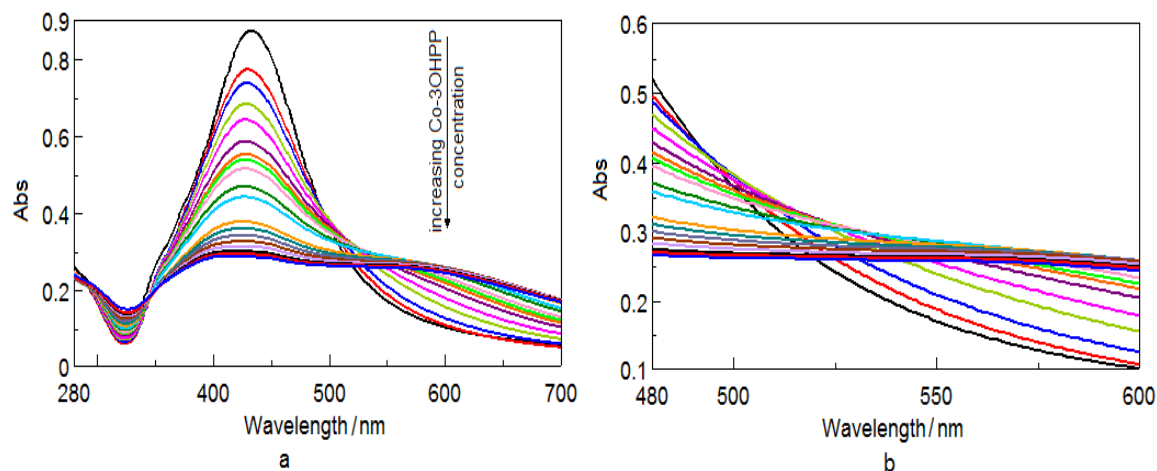


Fig. 3: Overlapped UV-vis spectra for the formation of *Co-3OHPP/nAg* hybrid by adding acidified metalloporphyrin to the Ag colloid (a). Detail of the isosbestic point at 525 nm (b).

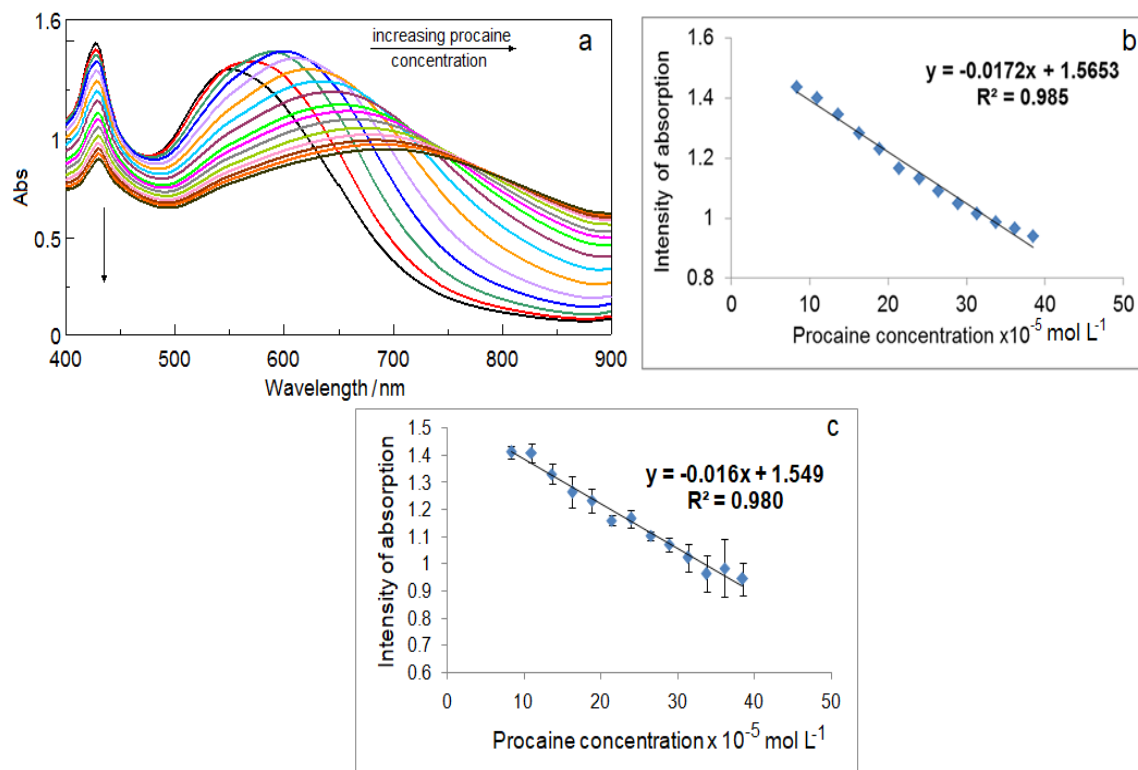


Fig. 4: Superposed UV-vis spectra recorded by adding of procaine to *Co-3OHPP/nAu* hybrid (a); the best dependence between the intensity of absorption and the concentration of procaine (b). Associated error bar after three independent experiments (c).

Analysing the UV-vis spectra (Fig. 4) it can be observed that during the adding of procaine to the *Co-3OHPP/nAu* hybrid solution the plasmon band is constantly shifting (in an almost linear fashion) to higher wavelengths ($\lambda = 571$ nm for $c = 2.802 \times 10^{-5}$ mol l⁻¹; $\lambda = 689$ nm for $c = 38.468 \times 10^{-5}$ mol l⁻¹) (Fig. 4a), proving that the phenomenon is not only due to dilution. The intensity of absorption is decreasing linearly with the increase in procaine concentration. This linear dependence is characterized by a correlation coefficient of 98.5% (Fig. 4b) for the procaine concentration domain of 8.35×10^{-5} mol l⁻¹ to 38.46×10^{-5} mol l⁻¹.

By adding procaine to the *Co-3OHPP/nAg* hybrid solution it can be observed in the UV-vis spectra (Fig. 5a) that the plasmon band is decreasing in intensity in a linear fashion with the increase in procaine concentration in a similar fashion with *Co-3OHPP/nAu* hybrid. The range of detected procaine concentration 5.39×10^{-5} mol l⁻¹ – 28.04×10^{-5} mol l⁻¹

is almost the same as in the case of gold hybrid and has an excellent correlation coefficient of 99.11% (Fig. 5b).

AFM analysis

The AFM was performed to compare the changes of the morphology of the two hybrid materials, *Co-3OHPP/nAu* and *Co-3OHPP/nAg* before and after being exposed to procaine.

The Co-porphyrin bearing hydroxyl-binding groups may generate several self-assembled architectures. As expected [24], AFM images proved that self-assembly into ordered triangular shapes is due to differences in electric charges (Fig. 6a-c and Fig. 7 g-i) whereas the less ordered geometrical shapes after treatment with procaine (Fig. 6 d-f and Fig. 7 j-l) are due probably to non-specific interactions between different molecules [27].

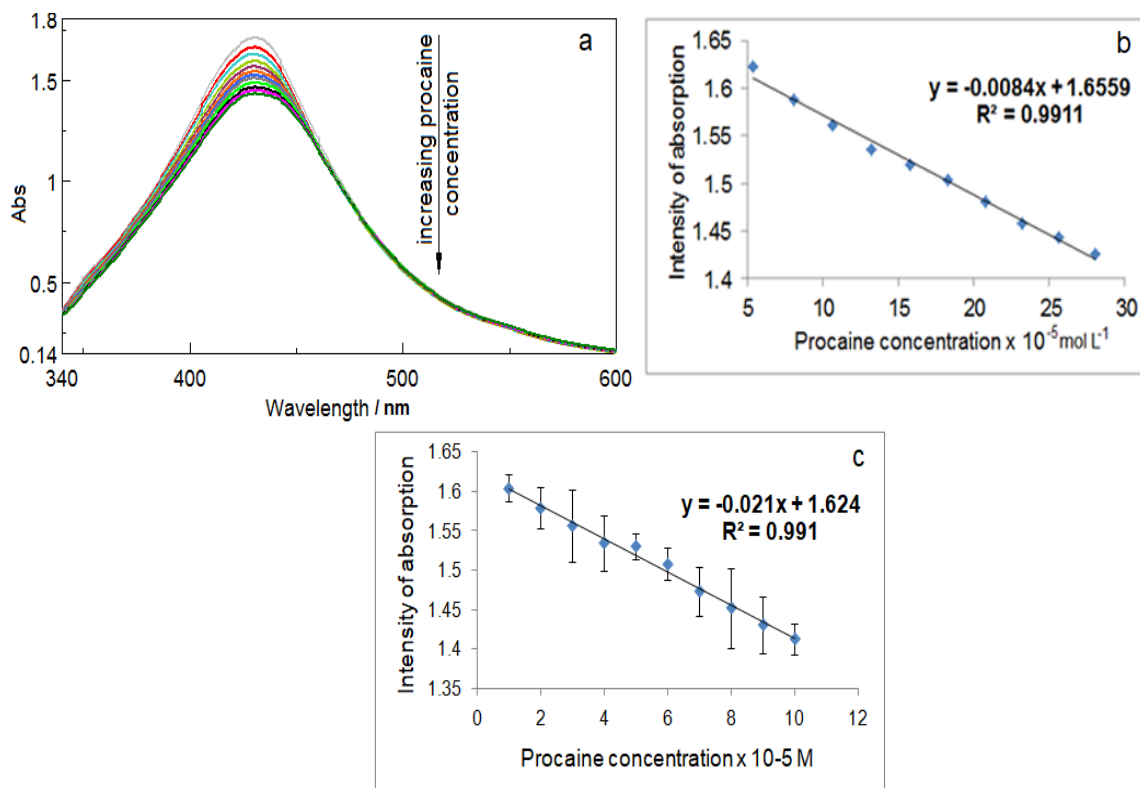


Fig. 5: Superposed UV-vis spectra by adding of procaine to *Co-3OHPP/nAg* hybrid (a); the best dependence between the intensity of absorption of the plasmonic band and the concentration of procaine (b). Associated error bar after three independent experiments (c).

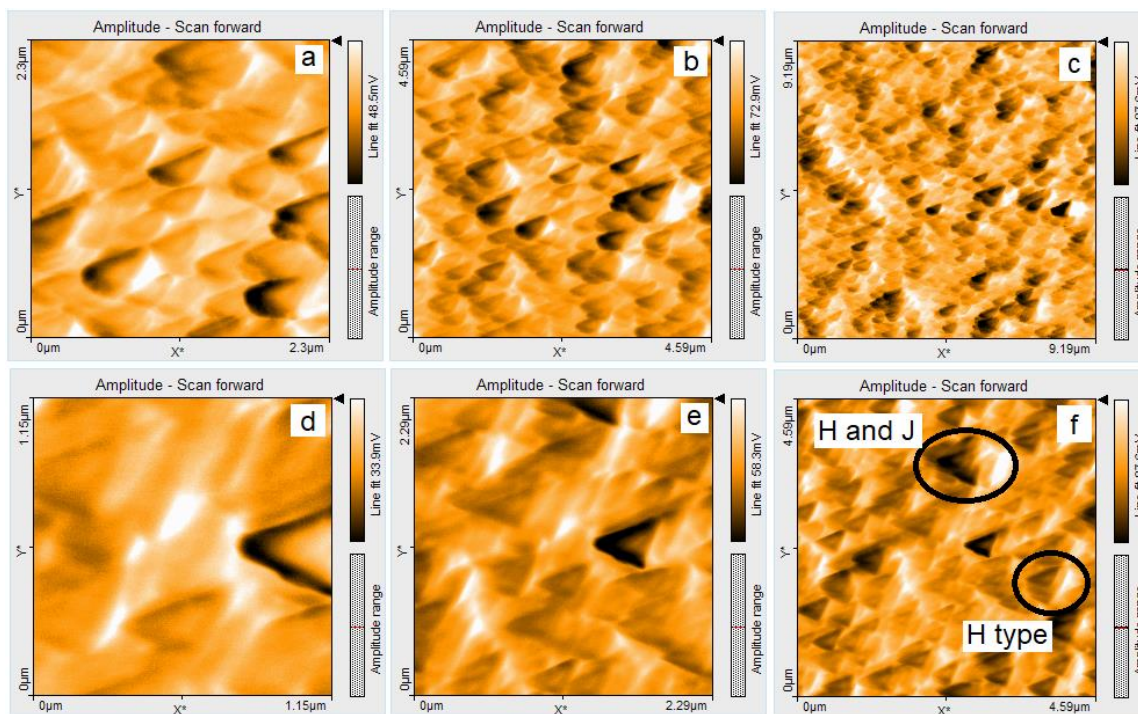


Fig. 6: AFM images for the *Co-3OHPP/nAu* hybrid before (a-c) and after treatment with procaine (d-f).

The AFM images of the *Co-3OHPP/nAu* hybrid treated with procaine (Fig. 6 d-f) show a similar size of triangular shaped particles (around 300 nm) that are evenly orientated and distributed in all the detected range. A J-type aggregation of particles is also visible (Fig. 6 f). Height distribution measured for 2 micrometers area is in the nanometric range 20.6 – 45 nm (Fig. 8 a).

AFM images of the *Co-3OHPP/nAg* hybrid treated with procaine (Fig. 7 j-l) present also the geometry of triangular shaped particles having in this case different smaller sizes varying from 100 nm to 250 nm. The triangular geometries are not very well

defined taking also the form of *kvatarons* (see AFM in Fig. 7 j and k dimension 1.15 μm x 1.15 μm and 2.29 μm x 2.29 μm), the name deriving from Abkhazian word *kvatar*, meaning ball, and these two coexisting forms are generating mixed aggregation. The aggregation phenomenon is more visible that in the case of the nAu hybrid, as the J-type aggregates are more bulky and thus higher (Fig. 7 k and l). Height distribution measured for 2 micrometers area is in this case in the range of 27.5 nm – 64 nm (Fig. 8 b). This result might be correlated with the better detection capacity of the silver hybrid toward procaine.

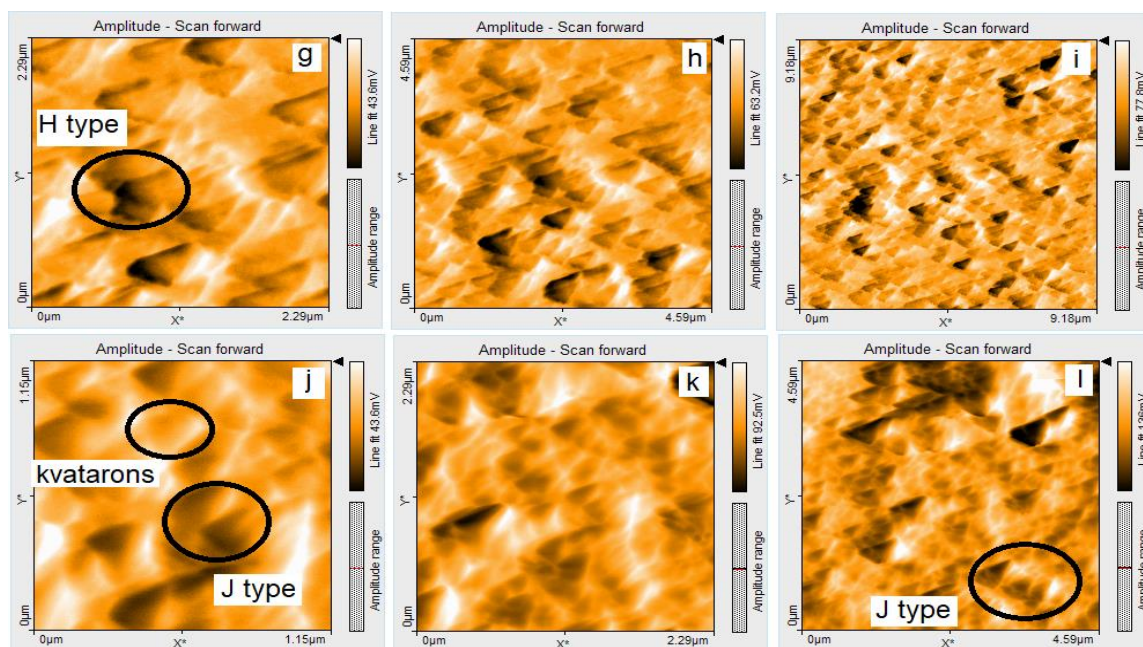


Fig. 7: AFM images for the *Co-3OHPP/nAg* hybrid before (g-i) and after treatment with procaine (j-l).

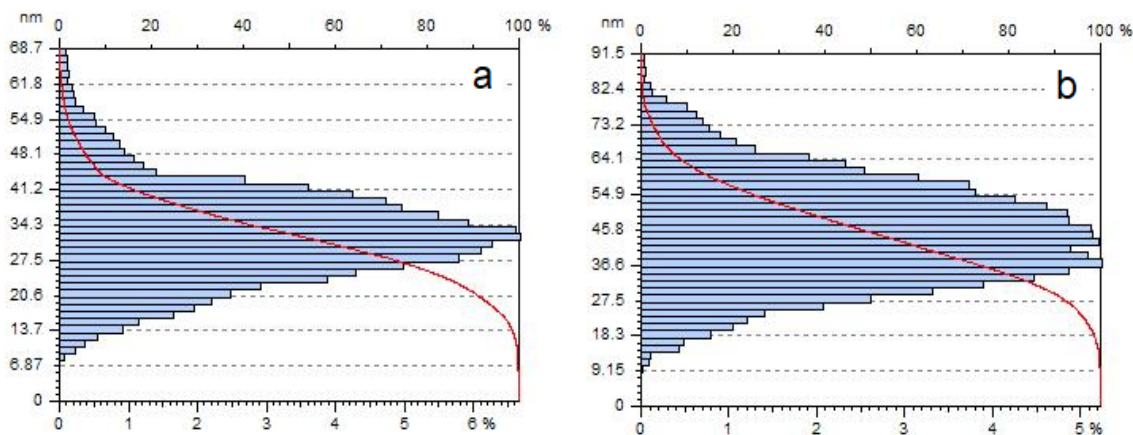


Fig. 8: Height distribution for the *Co-3OHPP/nAu* and *Co-3OHPP/nAg* hybrids after treatment with procaine.

Conclusions

Two hybrids *Co-3OHPP/nAu* and *Co-3OHPP/nAg* were obtained and tested for their ability to detect procaine in the concentration range that is relevant for the anesthetic remanence in post-operative control. Both hybrids present changes in UV-vis spectroscopy after interaction with procaine, in the same range of procaine concentration. The silver colloid is more easily obtainable and more economically affordable and its porphyrin hybrid has a wider range of detection from $5.39 \times 10^{-5} \text{ mol L}^{-1}$ to $28.04 \times 10^{-5} \text{ mol L}^{-1}$ procaine concentration. Besides, the plasmonic band is more clearly defined. AFM studies were performed to compare the morphology of the two hybrid materials, *Co-3OHPP/nAu* and *Co-3OHPP/nAg* after being exposed to procaine. Both materials display triangular geometries that in case of *Co-3OHPP/nAg* are not very well defined taking also the form of *kvatarons* and these two coexisting forms are able to generate pyramidal architectures.

Acknowledgements:

The authors from Institute of Chemistry Timisoara of Romanian Academy are kindly acknowledging the partial support of Romanian Academy, Program 3-Porphyrins/2017 and of UEFISCDI PNIII 107 PED/2017-COROXIPOR Project.

References

1. A. L. Sisk. Vasoconstrictors in local anesthesia for dentistry. *Anesth. Prog.*, **39**, 187 (1992).
2. V. A. Kral, C. Cahn, M. Deutsch, H. Mueller and L. Solyom. Procaine (Novocain) Treatment of Patients with Senile and Arteriosclerotic Brain Disease. *Canad. Med. Assoc. J.*, **87**, 1109 (1962).
3. A. Aslan, M. Dumitru and S. Galaftion. The Longitudinal Outpatient Treatment with Gerovital-H3. *Rom. J. of Geront. & Geriatrics*, **1**, 29 (1980).
4. S. Szatmári and D. Bereczki. Procaine treatments for cognition and dementia. *Cochrane Database Syst Rev.*, **4**, CD005993 (2008).
5. R. Henry and A. Morales. Topical lidocaine-prilocaine spray for the treatment of premature ejaculation: a proof of concept study. *Int. J. Impot. Res.*, **4**, 277 (2003).
6. A. Aslan, In *Theoretical of Aspects of Aging, Theoretical and practical aspects of chemotherapeutic techniques in the retardation of the aging process*, Academic Press, New York, p. 145 (1974).
7. T. Perls. The reappearance of procaine hydrochloride (Gerovital H3) for antiaging. *J. Am. Geriatr. Soc.*, **61**, 1024 (2013).
8. O. F. M. Sellevold, E. M. Berg and O. W. Levang. Procaine hydrochloride in cardioplegia (CPL): An effective drug in reducing postischaemic ventricular fibrillation in man, *Anesth. Analg.* **81**, 932 (1995).
9. Ö. Karadaş, F. Tok, S. Akarsu, L. Tekin and B. Balaban. Triamcinolone Acetonide vs Procaine Hydrochloride Injection in the Management of Carpal Tunnel Syndrome: Randomized Placebo-Controlled Trial. *J. Rehabil. Med.*, **44**, 601 (2012).
10. R. B. Salama and A. I. H. Omer. Colorimetric determination of procaine hydrochloride in pharmaceutical preparations. *J. Pharm. Sci.*, **69**, 346 (1980).
11. L. Vladescu, D. Moja, I. Badea and C. Ciomaga. Determination of Procaine hydrochloride by Potentiometric Titration. *Rev. Roum. Chimie*, **47**, 911 (2002).
12. L. Lei, X. Su, Q. Xie, J. He and S. Yao. A Novel Ion-Selective Sensor for Procaine Hydrochloride Based on a Piezoelectric Quartz Crystal Coated with a Procaine Tetraphenylborate PVC Membrane. *Mikrochimica Acta*, **134**, 63 (2000).
13. Y. T. He, J. D. Peng, J. X. Tang and C. Zhang. Incorporation of high performance liquid chromatography with resonance Rayleigh scattering detection for determination of procaine and lidocaine in human plasma. *Anal. Methods*, **5**, 7110 (2013).
14. W. A. Al-Uzri and M. I. Al-Heeti. Colorimetric Determination of Procaine hydrochloride in Pharmaceutical Preparations using Diazotization Coupling Reactions. *Int. J. Pharm. Tech. Res.*, **8**, 1042 (2015).
15. Y. H. Liao and J. C. Chou. Preparation and characterization of the titanium dioxide thin films used for pH electrode and procaine drug sensor by sol-gel method. *Mater. Chem. Phys.*, **114**, 542 (2009).
16. K. Tonooka, N. Naruki, K. Honma, K. Agei, M. Okutsu, T. Hosono, Y. Kunisue, M. Terada, K. Tomobe and T. Shinozuka. Sensitive liquid chromatography/tandem mass spectrometry method for the simultaneous determination of nine local anesthetic drugs. *Forensic Sci. Int.*, **265**, 182 (2016).
17. A. Saporito, L. Anselmi, A. Borgeat and J. A. Aguirre. Can the choice of the local anesthetic have an impact on ambulatory surgery perioperative costs? Chlorprocaine for popliteal block in outpatient foot surgery. *J. Clin. Anesth.*, **32**, 119 (2016).

18. S. Lin, C. S. Diercks, Y. B. Zhang, N. Kornienko, E. M. Nichols, Y. Zhao, A. R. Paris, D. Kim, P. Yang, O. M. Yaghi and C. J. Chang. Covalent organic frameworks comprising cobalt porphyrins for catalytic CO₂ reduction in water. *Science*, **349**, 1208 (2015).
19. H. Kon and T. Nagata. Syntheses, Properties, and Photoreactions of the Hybrid Molecules Consisting of a CoII Mononuclear Complex and Porphyrins. *Chem. Eur. J.*, **18**, 1781 (2012).
20. R. Arce, M. J. Aguirre and J. Romero. Sensor for quantitative analytical determination of sulphite in wine using a system of modified electrode and a membrane absorption system. *ECS Transactions*, **64**, 37 (2014).
21. E. Mazzotta and C. Malitesta. Electrochemical detection of the toxic organohalide 2,4-DB using a Co-porphyrin based electrosynthesized molecularly imprinted polymer. *Sens. Actuators B: Chemical*, **148**, 186 (2010).
22. A. Colombelli, M. G. Manera, V. Borovkov, G. Giancane, L. Valli and R. Rella. Enhanced sensing properties of cobalt bis-porphyrin derivative thin films by a magneto-plasmonic-opto-chemical sensor. *Sens. Actuators B: Chemical*, **246**, 1039 (2017).
23. S. Nardis, D. Monti, C. Di Natale, A. D'Amico, P. Siciliano, A. Forleo, M. Epifani, A. Taurino, R. Rella and R. Paolesse. Preparation and characterization of cobalt porphyrin modified tin dioxide films for sensor applications. *Sens. Actuators B: Chemical*, **103**, 339 (2004).
24. E. Fagadar-Cosma, I. Sebarchievici, A. Lascu, I. Creanga, A. Palade, M. Birdeanu, B. Taranu and G. Fagadar-Cosma. Optical and Electrochemical Behavior of New Nano-Sized Complexes Based on Gold-Colloid and Co-Porphyrin Derivative in the Presence of H₂O₂. *J. Alloys Compds.*, **686**, 896 (2016).
25. I. Creanga, G. Fagadar-Cosma, A. Palade, A. Lascu, C. Enache, M. Birdeanu and E. Fagadar-Cosma. New hybrid silver colloid-A₃B porphyrin complex exhibiting wide band absorption. *Dig. J. Nanomat. Bios.*, **8**, 561 (2013).
26. A. Palade, G. Fagadar-Cosma, A. Lascu, I. Creanga, M. Birdeanu and E. Fagadar-Cosma. New porphyrin-based spectrophotometric sensor for Ag⁰ detection. *Dig. J. Nanomat. Bios.*, **8**, 1013 (2013).
27. G. Bazzan, W. Smith, L. C. Francesconi, C. M. Drain. Electrostatic Self-Organization of Robust Porphyrin-Polyoxometalate Films. *Langmuir*, **24**, 3244 (2008).